

Cite this: *New J. Chem.*, 2011, **35**, 2773–2780

www.rsc.org/njc

PAPER

Phosphine stabilized copper(I) complexes of dithiocarbamates and xanthates and their decomposition pathways†

Mohammad Afzaal,^a Chico L. Rosenberg,^b Mohammad A. Malik,^c
Andrew J. P. White^b and Paul O'Brien*^c

Received (in Montpellier, France) 6th July 2011, Accepted 2nd September 2011

DOI: 10.1039/c1nj20586b

Phosphine stabilized compounds [Cu(I)(S₂CNEt₂)PR₃]₂ (**1–3**) (R = OMe, Me and Et, respectively) and [Cu(I)(S₂COEt)PR₃]₂ (**4, 5**), (R = OMe, and Me, respectively) have been prepared and characterised. The structures of compounds (**1–3**) were determined by X-ray single crystallography. The structures of all three compounds are based on centro-symmetric dimers which crystallise in the monoclinic space group P2₁/n with two [Cu(I)(S₂CNEt₂)PR₃]₂ molecules per unit cell. The thermal decomposition of selected complexes was investigated by thermogravimetric, differential scanning calorimetry and gas chromatography with mass spectroscopy to understand the possible decomposition pathways.

Introduction

The chemistry of dithiocarbamate (dtc) copper(II) complexes have been extensively studied,^{1–5} but there has been little research work into Cu(I) dtc's^{6–10} and even less into the chemistry of Cu(I) dtc's with coordinated Lewis base ligands.^{11,12} Although ligands which coordinate to metal ions *via* sulfur atoms are conventionally regarded as “soft” Lewis base donors and would therefore have a greater affinity for “soft” Lewis acids (*e.g.* Cu⁺), dithiocarbamates actually favour metal ions in higher oxidation states, stabilising copper(II) and even copper(III) species. The effect is conventionally held to be due to the extra partial negative charge on the sulfur atoms, arising from π -donation of the nitrogen atom's lone pair into π electron system of the –CS₂ group.^{13–15} Kowala and Swan¹¹ originally synthesised compounds of general formula [Cu(I)(S₂CNR₂)PEt₃] and [Cu(I)(S₂CNR₂)(PPh₃)₂] (where R = Me, Et, Pr and Bu) by the addition of one equivalent of PEt₃ or two equivalents of PPh₃ to solutions of the corresponding cuprous dialkyldithiocarbamates, which are yellow crystalline solids. These cuprous dialkyldithiocarbamates were in turn synthesised *via* a

combination of two previously reported methods, (i) the redox reaction of a *N,N,N'*-tetraalkyldithiuram disulfide with an excess of finely divided copper metal in CS₂⁸ and (ii) the reaction of cuprous halide or oxide¹⁰ with NaR₂NCS₂ in an organic solvent. Kowala and Swan simply dissolved and stirred the crude product made by method (ii)¹¹ in CS₂ with some copper metal powder until the solution became yellow. Since the aim of this method was to convert unwanted residual cupric dtc by-product into cuprous dtc, Victoriano and Cortes⁶ also synthesised Cu(I) dtc's in a similar manner by comproportionation of the appropriate Cu(II) dtc with powdered copper metal in CS₂. Recent studies have reported the formation of a highly symmetrical octanuclear complex containing a cube of Cu(I) centers; each face being occupied by a dithiocarbamate.¹⁶

Cu(I) xanthates were originally synthesised from copper(II) xanthate complexes. Unlike dtcs, xanthates favour copper in a low oxidation state, so once formed, the thermodynamically less stable Cu(II) xanthates undergo a redox decomposition to give the corresponding intense yellow/amber coloured insoluble Cu(I) complex together with dixanthogen (ROC(S)S–SC(S)OR).^{17,18} Although Cu(II) xanthates are thermodynamically less stable than Cu(I) xanthates; the latter are moisture and air-sensitive, reacting with O₂ and H₂O to regenerate copper(II) xanthate and Cu(OH)₂. The presence of Cu(II) thus catalyses the aerial oxidation of xanthate anions to dixanthogens, as subsequent decomposition of the copper(II) xanthate to copper(I) xanthate and dixanthogen remain; the latter being produced indefinitely if a continuous source of xanthate anions is supplied. The character of the xanthate anion is much more like that expected from sulfur donor Lewis base (*i.e.* “soft” and favouring lower oxidation state metal centres. In terms of resonant hybrids it can be said that, unlike

^a Center of Research Excellence in Renewable Energy, King Fahd University of Petroleum and Minerals, PO Box 1292, Dhahran, 31261 Saudi Arabia

^b Department of Chemistry, Imperial College of Science, Technology and Medicine, London, SW7 2AY, UK

^c School of Chemistry and School of Materials, The University of Manchester, Oxford Road, Manchester, M13 9PL, UK.
E-mail: paul.obrien@manchester.ac.uk

† Electronic supplementary information (ESI) available: Experimental details for GC-MS are given in Table S1. CCDC reference numbers 812045–812047. For ESI and crystallographic data in CIF or other electronic format see DOI: 10.1039/c1nj20586b

the dtc anion, the latter canonical form with more negative charge located on the sulfur atoms does not contribute that greatly to the overall electronic structure.¹⁹ This is evidenced by the O–CS₂ bond length and stretching frequency being closer to that of single O–C bonds (~ 1020 – 1280 cm⁻¹).²⁰

In this paper, we describe the preparation and characterisation of phosphorus ligand stabilised cuprous dithiocarbamates [Cu(I)(S₂CNEt₂)PR₃] (R = OMe (**1**), Me (**2**) and Et (**3**) and the xanthates [Cu(I)(S₂COEt)PR₃]₂ (R = OMe (**4**) and Me (**5**)). This is followed by the detail investigations into the thermal behaviour of compounds (**3**) and (**4**) in TGA, DSC and GC-MS experiments, leading to cuprous sulfide.

Results and discussion

The methods used for the preparation of cuprous diethyldithiocarbamate complexes with pendant PR₃ ligands (*i.e.* [Cu(I)(S₂CNEt₂)PR₃] in which R = OMe (**1**), Me (**2**) and Et (**3**)) were somewhat analogous to those employed in the synthesis of the ligand stabilised copper(I) β -diketonato complexes.^{21–23} (in which the PR₃ ligand was added to a suspension of CuCl to give an organically soluble adduct prior to addition of the sodium salt) and also the method of Kowala and Swan.¹¹ The synthesised compounds seem to be rather sensitive and it was found that the use of toluene as a solvent always seemed to cause decomposition of the dissolved compounds, whereas benzene solutions turned out to be stable. Differences in the character of complex (**1**) compared with the complexes (**2**) and (**3**) are highlighted in their NMR spectra, *i.e.* CH₃CH₂N peaks are at 1.04, 1.09 and 1.09 ppm and the CH₃CH₂S peaks are at 3.69, 3.79 and 3.79 ppm respectively. Closer inspection of the apparent multiplet at $\delta = 1.09$ ppm in the ¹H NMR spectrum of (**3**) reveals that it is in fact two triplets 1.11 and 1.08 ppm which correspond to the CH₃CH₂P and CH₃CH₂N protons. High values for ¹H NMR of the PPH₃ analogue of these complexes (at 3.88 and 1.20 ppm) are due to the use of CDCl₃ as a solvent.⁶

The methods used for the preparation of cuprous *O*-ethylxanthates with pendant PR₃ ligands (*i.e.* [Cu(EtOCS₂)PR₃]₂, in which R = OMe (**4**) and Me (**5**) were similar to those used for the cuprous dtc complexes. Unlike the NMR spectra of the dtc compounds, no clear trends in the chemical shifts are notable for these xanthate complexes and similarities between trialkylphosphine complexes *versus* the phosphite complex are not highlighted either. The only signal out of ¹H and ¹³C spectra of both complexes which seems significantly different from the other equivalent signals is the CH₃CH₂O quartet of (**5**) at $\delta = 1.40$ ppm, while the equivalent signals for (**4**) is at 1.06 ppm.

The molecular structures of compounds (**1**)–(**3**) are shown in Fig. 1–3 respectively and selected bond lengths and angles are given in Table 1. All three structures are centro-symmetric and have a distinctive Cu₂S₄C₂ core with a chair confirmation. This motif is directly analogous to the Cd₂O₂S₂C₂ units present in the cadmium monothiocarbamate polymer structure {Cd(SOCNEt₂)₂}_n.²⁴ In the present three structures, in all cases the central Cu₂S₂ “ring” is planar and the CuS₂C “ring” is folded out of this plane by *ca.* 78, 72 and 73° in (**1**), (**2**) and (**3**) respectively. The only related Cu₂S₄C ring system

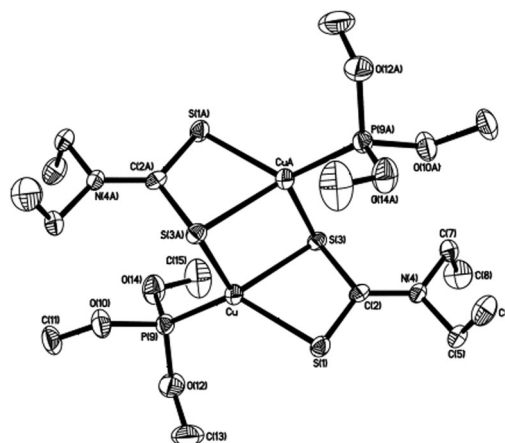


Fig. 1 The molecular structure of the C₁-symmetric complex (**1**) (50% probability ellipsoids).

Table 1 Comparative selected bond lengths (Å) and angles (°) for **1**, **2** and **3**

Complex	1	2	3
Cu–S(1)	2.3488(9)	2.3638(15)	2.3501(9)
Cu–S(3)	2.4657(9)	2.4870(14)	2.5794(9)
Cu–P(9)	2.1703(10)	2.2070(15)	2.2078(9)
Cu–S(3A)	2.3920(9)	2.3846(14)	2.3729(9)
Cu···CuA	2.9141(9)	2.6725(14)	2.6181(8)
S(1)–C(2)	1.714(3)	1.699(5)	1.719(3)
C(2)–S(3)	1.752(3)	1.740(4)	1.741(3)
C(2)–N(4)	1.320(4)	1.326(6)	1.334(4)
S(3)···S(3A)	3.8872(15)	4.074(2)	4.2088(16)
S(1)–Cu–S(3)	75.20(3)	74.38(4)	73.57(3)
S(1)–Cu–P(9)	129.88(4)	126.66(6)	128.43(4)
S(1)–Cu–S(3A)	105.76(3)	110.84(5)	110.27(3)
S(3)–Cu–P(9)	120.74(4)	118.27(6)	111.75(3)
S(3)–Cu–S(3A)	106.29(3)	113.50(4)	116.33(2)
P(9)–Cu–S(3A)	112.52(3)	109.32(5)	111.52(3)
Cu–S(3)–CuA	73.71(3)	66.50(4)	63.67(2)

in the literature is that in the structure of *bis*(μ_2 -*N,N*-diethyldithiocarbamate)-di-copper(I) where the 8-membered ring adopts a twisted boat conformation with a transannular Cu···Cu separation of 2.756 Å.²⁵ The most noticeable and interesting feature in these structures is the effect on the ring geometries of the electron-withdrawing or -donating nature of the substituents on the phosphorus atoms. In (**1**), which contains electron withdrawing methoxy groups, we see the largest Cu···CuA separation (2.9141(9) Å), whereas in (**2**) and (**3**), which have progressively greater electron donating substituents, Cu···CuA distance (Table 1) reduces to 2.6725(14) and 2.6181(8) Å respectively (the associated transannular S(3)···S(3A) separations are 3.887, 4.074 and 4.208 Å respectively). Accompanying these differences are marked variations in the angles at Cu and S(3) within the central 4-membered ring, the angle at copper ranging between 106.29(3) in (**1**) and 116.33(2)° in (**3**) with those at S(3) (and S(3')) being between 73.71(3) in (**1**) and 63.67(2)° in (**3**). Although the difference between the Cu–S(1) and Cu–S(3) distances become progressively greater as one goes from structure (**1**) to structure (**3**), it can be considered that in each case the diethyldithiocarbamate ligand binds in a μ_2 - η^2 -fashion, with S(3) adopting the binucleating role. Similar

asymmetries on Cu–S distances have also been observed in other dtc complexes of copper (*e.g.* bis(tetraethylammonium)-bis((μ_3 -selenido)(μ_2 -selenido))-tris(*N,N*-diethyldithiocarbamato)-tri-copper-molybdenum²⁵).

Clearly in (3) the Cu–S(3) linkage is appreciably weakened and that between Cu and CuA strengthens (Table 1). Thus, the copper centres can be considered as adopting severely distorted tetrahedral coordination geometries with angles in the ranges 75.20(3)–129.88(4)° for (1), 74.38(4)–126.66(6)° for (2) and 73.57(3)–128.43(4)° for (3), the most acute angle in each case being associated with the bite of the diethyldithiocarbamato ligand. In (1), (2) and (3) the copper atom lies 0.45, 0.49 and 0.42 Å respectively out of the P, S(1), S(3A) plane in the direction of S(3). Although there is a marked lengthening of the Cu–P bond on going from structure (1) to (2) (2.170(3) *cf.* 2.207 Å, there is no significant difference on going from (2) to (3), where the Cu–P distance is 2.207(8) Å. In none of the structures are there any intermolecular interactions of note.

Thermal studies of [Cu(I)(S₂CNEt₂)PEt₃] (3)

Compounds (3) and (4) were analysed by DSC and TGA experiments (from ~30–500 °C). For compound (3) with increasing temperature, the first change was indicated by an endothermic trough in DSC plot at ~74.7 °C, corresponding to the melting point (~69.0 °C by mp apparatus) (Fig. 4). The remaining DSC plot was also endothermic, indicative of further degradation on the compound, its peak and troughs paralleling those in TGA plot, which indicated five main, overlapping periods of weight loss over the entire temperature range (a–e, Fig. 4). The first three periods of weight loss (a, b and c), which occur over the temperature ranges ~122–202, ~202–234 and ~234–256 °C account for ~16.9%, ~11.6% and ~8.5% consecutive decreases in weight respectively (total of ~37%), corresponding to the loss of the PEt₃ ligands (theoretically 35.8%). This process is seen in the DSC plot (after the melting trough) as a fairly steady endothermic decrease that slows quite abruptly at the DSC peak at 253 °C. The first period of weight loss (a; ~16.9%) roughly corresponds to the initial loss of half the PEt₃ ligands (theoretically ~17.9%). Why the loss of the remaining ligands should seem to occupy two periods (b and c) is not clear, but these two

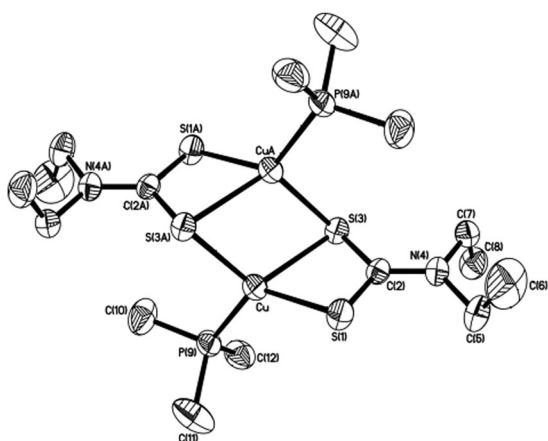


Fig. 2 The molecular structure of the C₁-symmetric complex (2) (30% probability ellipsoids).

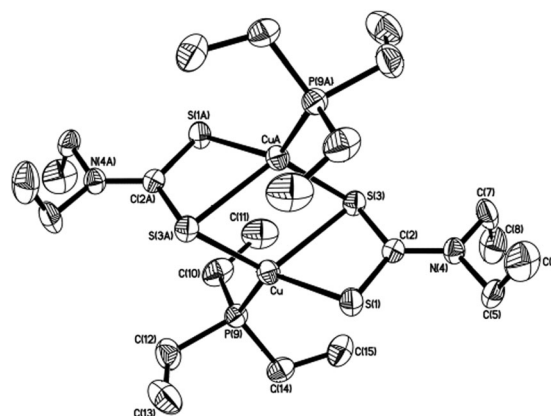


Fig. 3 The molecular structure of the C₁-symmetric complex (3) (50% probability ellipsoids).

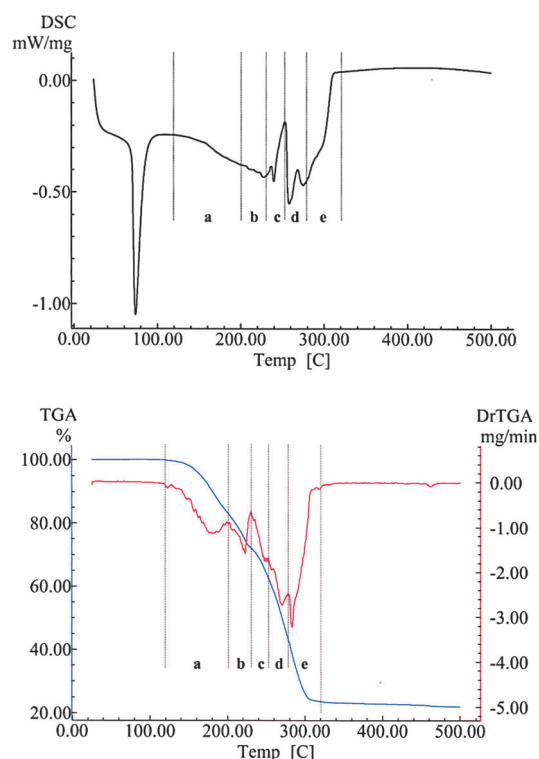


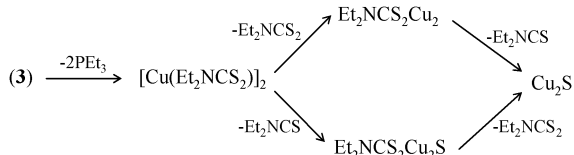
Fig. 4 DSC (TOP) and TGA (bottom) of complex (3) as a function of temperature.

periods are not that well defined (especially c) and there are probably other decomposition processes also starting to occur. Indeed, this is indicated in the DSC by the “peak” at ~253 °C; if PEt₃ ligand loss and subsequent thermal degradation processes were separated by a wider temperature range, the aforementioned peak would instead be a baseline plateau.

Minor fluctuations in the DSC and TGA plots over the fourth period of weight loss (d; ~256–280 °C) seem to roughly coincide with each other. The % weight loss for the fourth and fifth periods, d and e, are ~20.5% and 19.3% respectively (*i.e.* ~39.8% in total). These figures correspond to the net loss of Et₂NCS and Et₂NCS₂ fragments (theoretically 17.6% and 22.5% each; 40.1% in total) over these two final stages (d and e) to leave a residue with 23.5% of the mass of the starting sample.

This corresponds fairly well to the overall decomposition of (3) to Cu_2S (theoretically 24.1%).

Since the two weight losses **d** and **e** are quite close (20.5 and 19.3%), this tends to suggest that although dtc fragments are lost sequentially from the $[\text{Cu}(\text{S}_2\text{CNEt}_2)_2]_2$ dimer, there is an approximately even probability that the first will leave as either an Et_2NCS or an Et_2NCS_2 fragment. Additionally, for a given residual molecule after stage **d**, the loss of the second dtc fragment is necessarily of the alternative type to the first one to leave behind a residue of Cu_2S . The decomposition process can thus be summarised as:



To gain further information about the thermal behaviour, GC-MS of compound (3) is also carried out. Mass spectra were taken at retention times t (minutes) = 8:05 (**a**), 30:30 (**b**), 34:35 (**c**), 40:42 (**d**) and 43:48 (**e**), the latter two corresponding to the two largest peaks in the GC trace (the first peak at $t = 2:18$ min corresponds to the solvent coming through the column first).

Mass spectrum (**a**) shows a peak at $m/z = 118$, indicating initial dissociation of PEt_3 at injection, which pass through the column quite rapidly as this peak is not seen in any of the subsequent mass spectra. Peaks at $m/z = 90$ and 62 in (**a**) correspond to the fragmentation of PEt_3 into the HPEt_2 and the H_2PEt respectively. Additionally, there are peaks at 103 and 75 due to loss of CH_3 from PEt_3 an HPEt_2 .

Spectra (**b**) to (**e**) share many peaks, the presence and assignment of which are summarised in Table 2. They each have a major peak at 116, which is indicative of an Et_2NCS fragment. This peak is accompanied in each case with peaks at 88 and 60, which can be attributed to the loss of one or two C_2H_4 groups from this fragment. A peak at $m/z = 100$ is also present in spectra (**b**) and (**c**) and is tentatively assigned to the loss of CH_4 from the Et_2NCS fragment. Likewise, the peak at 72 seen in spectra (**b**) to (**d**) could also be due to the loss of CH_4

Table 2 Presence and assignment of major peaks in mass-spectra (**b**)–(**e**) in GC-MS study of compound **3**

Peak assignment (mass m/z)	Retention time t (minutes)	(b) (30:30)	(c) (34:35)	(d) (40:42)	(e) (43:48)
H_2NCS	(60)	✓	✓	✓	✓
CH_2NCS , ^a Et_2N	(72)	✓	✓	✓	✓
EtNHCS	(88)	✓	✓	✓	✓
$\text{HCN}(\text{Et})\text{CS}^a$	(100)	✓	✓	✓	✓
Et_2NCS	(116)	✓	✓	✓	✓
EtNCS_2 / EtNCS_2H^a	(148/149)	✓	✓	✓	✓
$\text{Et}_2\text{NCS}_2\text{Et}^a$	(177)	✓	✓	✓	(✓ 178)
$\text{Et}_2\text{NCS}_2\text{CNEt}^a$	(203)	✓	✓	✓	✓
$\text{Cu}(\text{S}_2\text{CNEt}_2)$	(212)	✓	✓	✓	✓
$(\text{S}_2\text{CNEt}_2)_2$	(232)	✓	✓	✓	✓
$\text{Cu}(\text{S}_2\text{CNEt}_2)_2$	(359)	✓	✓	✓	✓
$[\text{Cu}(\text{S}_2\text{CNEt}_2)]_2$	(422, 424)	✓	✓	✓	✓

^a Tentative assignment.

from the EtNHCS fragment ($m/z = 88$), although this mass also coincides with that of the fragment Et_2N . Also seen in spectra (**b**) to (**d**) are a cluster of peaks around $m/z = 149$ which could correspond to the whole Et_2NCS_2 ligand ($m/z = 148$) or a protonated form of it. These spectra also contain some higher signals at $m/z = 177$, 203 and 232, which are probably due to combined fragments of Et_2NCS_2 ligands.

The most notable aspects of this experiment are the clusters of peaks seen in (**d**) and (**e**) at around $m/z = 212$, 359 and 422/424 which correspond to the Cu containing fragments $\text{Cu}(\text{S}_2\text{CNEt}_2)$, $\text{Cu}(\text{S}_2\text{CNEt}_2)_2$ and $[\text{Cu}(\text{S}_2\text{CNEt}_2)]_2$ respectively; the former clearly a fragment of either of the latter two species. $\text{Cu}(\text{S}_2\text{CNEt}_2)_2$ could arise from decomposition/fragmentation of the ‘parent ion’ $[\text{Cu}(\text{S}_2\text{CNEt}_2)]_2$ since both peaks are seen together in (**d**) and (**e**). However, it could also be indicative of earlier decomposition of compound (3) via disproportionation after the loss of PEt_3 ligands. The cluster of peaks at $m/z = 422$ and 424 (*i.e.* $[\text{Cu}(\text{S}_2\text{CNEt}_2)]_2$) also has a smaller peak at 426, their relative intensities being approximately 3:3:1 respectively. This rough matches the ratio $\sim 5:4:1$, which is expected for M^+ species containing two copper atoms, arising due to the relative abundance’s of the isotopes ^{63}Cu and ^{65}Cu (~ 69 and 31% respectively).

The origin of the two closely spaced but distinct peaks in the GC trace at t (minutes) = 40:42 and 43:48 is somewhat curious because their corresponding mass spectra ((**d**) and (**e**)) are broadly similar. However, since both spectra show a ‘parent ion’ at around 424 (*i.e.* $[\text{Cu}(\text{S}_2\text{CNEt}_2)]_2$, possibly a ‘‘chair’’ isomer (with C_i point symmetry, as seen in the crystal structure of the compound) and a ‘‘boat’’ isomer (with C_2 point symmetry). If this were indeed the case then it should appear that the coordination of a phosphite ligand locks the $\text{Cu}_2\text{S}_4\text{C}_2$ cycle into the ‘‘chair’’ confirmation in the solid state. The study seems to indicate partial decomposition at the start of the experiment with continuous decomposition during it, since Et_2NCS_2 and its fragments are seen continuously throughout the course of the experiment.

Thermal studies of $[\text{Cu}(\text{I})(\text{S}_2\text{COEt})(\text{P}(\text{OMe})_3)]$ (**4**)

DSC, TGA and GC-MS studies of compound (**4**) (Fig. 5) were also carried out. The first change with increasing temperature seen in the DSC of (**4**) was a melting endotherm at ~ 72 °C. This temperature also heralded the start of the first gradual period of weight loss observe in the TGA up to ~ 121 °C of $\sim 13.1\%$. The latter temperature is fairly close to the reported decomposition temperature for (**4**) of ~ 127.5 °C as determined by mp apparatus. The 13.1% weight loss could be accounted for by the loss of $\frac{1}{2}$ equiv. of CS_2 (theoretically 12.3%), which has been previously reported as an initial product from the thermal decomposition of the metal xanthates (including those of copper), although this initial period of weight loss is also likely to include the loss of some $\text{P}(\text{OMe})_3$ ligand too.

The only other major endothermic region in the DSC occurs over the temperature range (~ 140 – 185 °C), coinciding with a continuous loss of mass (a further $\sim 60.8\%$) in the TGA. Smaller, irregular endothermic troughs from ~ 140 – 160 °C are roughly matched by a slight shoulder seen on the major

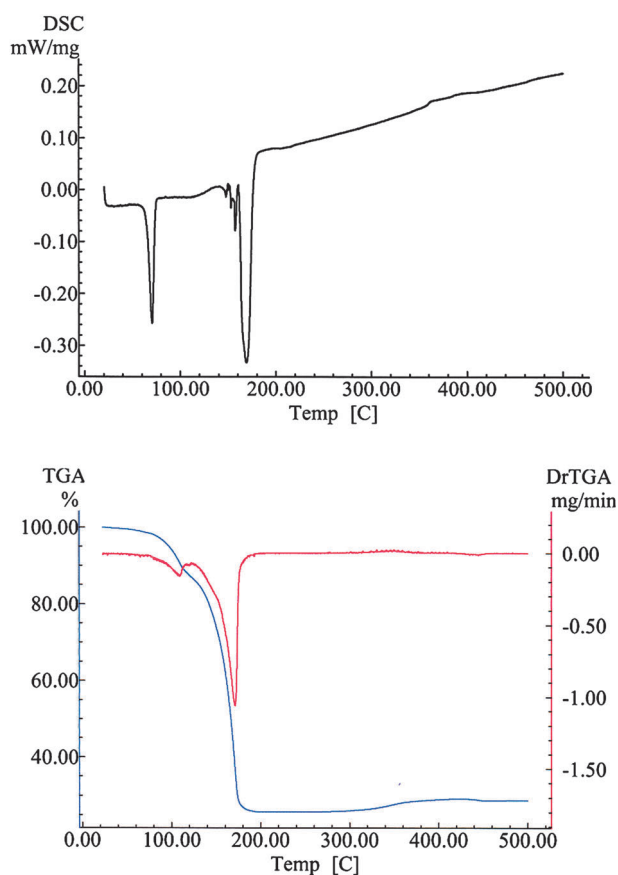


Fig. 5 DSC (TOP) and TGA (bottom) of complex (4) as a function of temperature.

downward peak in the TGA first derivative plot. This data shows the decomposition of (4) to be complete by $\sim 190^\circ\text{C}$, leaving a residue with $\sim 26.1\%$ of the mass of the starting sample (*i.e.* total observed weight loss of $\sim 73.9\%$), which corresponds to the formation of Cu_2S (theoretically 25.8%). This compound was also formed after thermal decomposition of compound (3) but only after heating to a considerably higher temperature (300°C at a heating rate of $10^\circ\text{C min}^{-1}$; in repeat runs of (4) at this faster heating rate, complete decomposition was observed by $\sim 225^\circ\text{C}$).

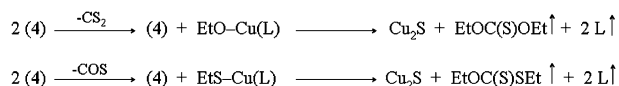
The GC trace of compound (4) shows a peak corresponding to the solvent coming through the column, mainly occurs over retention times t (minutes) = $0:30$ – $1:30$, but has a slightly shoulder from $\sim 1:30$ – $3:30$ min and gradually falls off to ~ 10 min. This probably accounts for emergence of the ligand $\text{P}(\text{OMe})_3$ from the column, although no mass spectra were taken at these earlier retention times. Times at which mass spectra were taken corresponded to a range of GC peaks seen between $\sim 21:55$ and $\sim 47:06$ min, including most of a series of small GC peaks seen between ~ 27 – 49 min that were spaced at fairly regular intervals (~ 2 – 3 min). The mass spectra in this series were broadly similar (*i.e.* MS peaks with the same m/z values were seen, although their relative intensities varied). These were thought to be the result of an impurity in the column. The two peaks at retention times $t = 21:55$ and $30:20$ min seem conspicuously independent of the aforementioned series of smaller peaks; apart from being the most

prominent peaks in the GC (after the large solvent peak at the start). However, there did not appear to be any copper species present in their corresponding mass spectra (*i.e.* no group of peaks with relative height ratios and differences in m/z corresponding to the relative abundance of different copper isotopes were seen). This is probably due to the lower decomposition temperature of the $\text{Cu}(\text{I})$ xanthates (lit. $\sim 120^\circ\text{C}$,²⁶) but seen to occur over ~ 80 – 190°C from TGA and DSC of (4), which means that, unlike with dtc's, complete decomposition occurs at injection to produce some solid copper containing residue (*e.g.* Cu_2S), while the decomposition of by-products of the ligands pass down the column

The m/z values (with their respective assignments) for the major peaks in the $t = 21:55$ min mass spectrum are 40 (C_2O or C_3H_4), 108 (EtS_2CH_3 , $\text{C}_3\text{H}_8\text{O}_2\text{S}$ or $\text{C}_2\text{H}_4\text{OS}_2$), 183 ($\text{EtOC}(\text{S})\text{S}_2\text{Et}$) and 262 (largest peak; $\text{EtOCS}_2)_2\text{H}_4\text{O}$ or $(\text{EtO})_2\text{S}_5$); and for the $t = 30:20$ min mass spectrum they are 57 (EtOC), 71 ($\text{C}_3\text{H}_3\text{O}_2$ or $\text{C}_3\text{H}_3\text{S}$), 112 ($\text{C}_6\text{H}_8\text{O}_2$ or $\text{C}_6\text{H}_8\text{S}$), 113 ($\text{C}_6\text{H}_9\text{O}_2$ or $\text{C}_6\text{H}_9\text{S}$), 149 (largest peak; $\text{EtOC}(\text{S})\text{SEt}(-\text{H})$), 167 ($\text{EtOC}(\text{S})\text{SOEt} (+\text{H})$ or $\text{EtOC}(\text{S})\text{SCSH} (+\text{H})$ and 279 ($\text{EtOC}(\text{S})\text{SOEt} (+\text{C}_6\text{H}_9\text{O}_2$ or $+\text{C}_6\text{H}_9\text{S})$).

The solubility problems associated with these compounds would appear to arise from loss of ligands to leave the insoluble solid $\text{Cu}(\text{I})\text{S}_2\text{COEt}$, necessitating the addition of further ligand to the solvent to form a soluble, kinetically stable complex. However, since the microanalysis of complexes (4) and (5) indicate the appropriate $\text{Cu}(\text{S}_2\text{COEt})\text{PR}_3$ stoichiometry, it follows that the loss of solubility over time of (4) and (5) may arise from a re-arrangement in the solid state from a kinetically stable molecular complex to a thermodynamically stable polymeric structure. Fragments with high m/z values are seen in the FAB mass spectra of these compounds, which could be indicative of a polymeric structure (xanthate anions are also known to coordinate to other transition metals in a bridging mode, *e.g.* cobalt and nickel),²⁸ but this is by no means conclusive. Unfortunately, no solid crystalline samples of xanthates could be prepared.

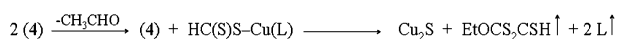
From the TGA, DSC and GC-MS data, the thermal decomposition of (4) appears to be slightly more complex, since the secondary decomposition products that would be expected/required for leaving a residue of Cu_2S from such a mechanism (*e.g.* EtOH , EtSH or RS-SR) are not seen in the GC-MS, which also shows some considerably heavier species. Also, the initial weight loss in the TGA of $\sim 13.1\%$ only corresponds to an initial loss of approximately half an equivalent of CS_2 (1 equiv. = 24.6%) or approx. $\frac{2}{3}$ equiv. of COS (Th. 1 equiv. = 19.4%). However, two feasible decomposition pathways that involve fractional loss of CS_2 or COS (both a $\frac{1}{2}$ equiv.) are:



The TGA data and the GC-MS results respectively support these pathways. As mentioned previously, the loss of half an equivalent of CS_2 (Th. 12.3%) is roughly reflected in the first TGA mass loss (obs. 13.1%), although the other decomposition by-product, $\text{EtOC}(\text{S})\text{OEt}$ ($m/z = 134$), is not seen in any mass

spectra. Conversely, the loss of a half equivalent of COS (Th. 9.7%) in the second pathway is not supported by the initial TGA loss, but it is by the GC-MS data because the by-product EtOC(S)SEt ($m/z = 150$) is indeed seen as the major signal in the mass spectrum for the second GC peak ($m/z = 149$; EtOC(S)SEt(-H)). In view of the possibility that partial loss of P(OMe)₃ may account for some of the initial TGA weight loss, the latter path would seem more likely, although this is by no means conclusively.

Another decomposition mechanism, which is tenuously supported by the GC-MS data and has also been observed in the decomposition of alkylxanthate complexes of other metals,^{27,28} involves the initial loss of an aldehyde molecule to leave an intermediate species in which the group HCS₂⁻ is coordinated to the metal centre. Although no signal corresponding to acetaldehyde was observed in any mass spectra (it would, after all, be expected to elute quite rapidly), a signal was seen at $m/z = 167$, which could correspond to the fragment EtOCS₂CSH (+H). This could conceivably arise from the reaction of the aforementioned intermediate species with an adjacent, un-decomposed xanthate anion/molecule of (4):



The theoretical weight loss for an initial loss of $\frac{1}{2}$ equiv. acetaldehyde = 7.1%, which, if accompanied by some preliminary P(OM)₃ loss, could fit with the first weight loss observed in the TGA (13.1%). In addition, the MS peak at $m/z = 167$ has an intensity of 62% of that of the peak at $m/z = 149$, which corresponds to EtOC(S)SEt (-H) formed in the proposed mechanism involving $\frac{1}{2}$ equiv. COS loss, so it is also feasible that these decomposition pathways occur in competition with each other.

Conclusions

Ligand stabilised cuprous dithiocarbamate and xanthate complexes were formed when phosphorus donor ligands were used. The solid xanthates eventually become insoluble unless excess phosphorus ligand was present. The dithiocarbamate complexes were found to be somewhat unstable and difficult to handle, eventually decomposing on standing at ambient temperatures to produce dark, copper(II) species, particularly in solution. Thermal studies indicate that both compounds (3) and (4) decompose at low temperature (*i.e.* ~120–320 °C and ~150–230 °C for (3) and (4) respectively) to produce cuprous sulfide.

Experimental section

General

All reactions and manipulations were carried out under an atmosphere of argon using standard Schlenk techniques. All reagents were purchased from Sigma Aldrich Ltd and were used and stored as supplied with no further purification. In general, anhydrous solvents were obtained by distillation over an appropriate drying agent. Melting points were recorded in

sealed tubes using an electrothermal melting point apparatus and were uncorrected. ¹H, ¹³C and ³¹P solution NMR spectra were recorded at 400 MHz at ambient temperatures on a DRX-400 in benzene-d₆. Reference for ³¹P was H₃PO₄. CHN microanalyses were either out at the analytical laboratories at the University of North London or at the Department of Chemistry's elemental analysis service at University College London. DSC was carried out on a Shimadzu DSC-50 at heating rates of 10 °C min⁻¹ (for compounds (3) and (4)) and 2 °C min⁻¹ (for compound (4)), with a rate flow of 30 cm³ min⁻¹ in all instances. TGA was carried out on a Shimadzu TGA-50 at heating rates of 10 °C min⁻¹ (for compounds (3) and (4)) and 2 °C min⁻¹ (for compound (4)), with a rate flow of 60 cm³ min⁻¹ in all instances. For TGA and DSC studies, the compounds were pressed into aluminium cells under a nitrogen atmosphere in a glove box. GC-MS analysis of compounds (3) and (4) were carried out using a Hewlett-Packard Series II HP5890 gas chromatograph integrated with a JEOL JMS AX505W mass spectrometer. Samples were prepared by dissolving the compounds (30–50 mg) in dry benzene (0.5 cm³). Experimental details and instrumentation for GC-MS is given in supporting information (Table S1†).

X-Ray structure determination

The data for **1**, **2** and **3** were collected using Siemens P4 diffractometers, each fitted with a single point detector (scintillation counter) and a conventional sealed tube X-ray source (Table 3).† For instruments of this type there is a close relationship between the number of data collected and the data collection time (a relationship that is broken for area detector systems such as CCDs or, earlier, film). Additionally, when using copper-based X-rays the drive time between data points as the 4-circle goniometer repositions itself also adds significantly to the overall data collection time. Consequently, it is a typical approach for such instruments to restrict the resolution of the data collection when using copper radiation, and experience suggested 0.89 Å to be a practical choice. Increasing this to 0.84 Å would typically double the data collection time with the addition of only a small percentage of observed data, and so was not a justifiable approach. Hence, the check CIF report complains of low resolution data for **1** and **2**. The compactness of the data set for **3** (because of the use of molybdenum-based X-rays), combined with the much larger crystal size (note that the instrument was fitted with a 1 mm collimator) meant that, contrary to the situation for **1** and **2**, data could be collected to a resolution of 0.84 Å in a reasonable time.

The cabinet of the diffractometer used for the data collection of **2** was physically unable to accommodate a low temperature device, so this data collection was indeed undertaken at room temperature. “The PMe₃ group in the structure of **2** was found to be disordered. Two orientations were identified for the methyl carbon atoms of *ca.* 80 and 20% occupancy, geometries were optimised (with all six P–C distances, and all six C–P–C angles, restrained to be similar), the thermal parameters of adjacent atoms were restrained to be similar and only the non-hydrogen atoms were refined anisotropically (those of the minor occupancy orientation were refined isotropically).”

Table 3 Experimental and refinement details for the X-ray structures of compounds 1–3

Complex	(1)	(2)	(3)
<i>Fw</i>	C ₁₆ H ₃₈ N ₂ O ₆ P ₂ S ₄ Cu ₂	C ₁₆ H ₃₈ N ₂ P ₂ S ₄ Cu ₂	C ₂₂ H ₅₀ N ₂ P ₂ S ₄ Cu ₂
<i>M</i>	671.74	575.74	659.90
Temperature (K)	203	293	183
Crystal system	Monoclinic	Monoclinic	Monoclinic
Space group	<i>P</i> 2 ₁ / <i>n</i> (no. 14)	<i>P</i> 2 ₁ / <i>n</i> (no. 14)	<i>P</i> 2 ₁ / <i>n</i> (no. 14)
<i>a</i> (Å)	10.7684(4)	10.1476(6)	11.0675(12)
<i>b</i> (Å)	11.9449(6)	12.1434(8)	11.4557(13)
<i>c</i> (Å)	11.2266(6)	12.1663(9)	12.6537(17)
β (°)	96.833(2)	111.287(4)	92.088(8)
<i>V</i> (Å ³), <i>Z</i>	1433.79(12), 2	1396.92(17), 2	1603.3(3), 2
<i>D_c</i> (g/cm ^{−3})	1.556	1.369	1.367
Max. and min. transmission	0.7263 and 0.2782	0.1992 and 0.0894	0.3479 and 0.2349
<i>R</i> ₁ (obs), <i>wR</i> ₂ (all)	0.0334, 0.0840	0.0512, 0.1413	0.0353, 0.0804
Largest difference peak/hole /e Å ^{−3})	0.489 and −0.387	0.662 and −0.432	0.333 and −0.276

CCDC 812045–812047 contain the supplementary crystallographic data for this paper.

Synthesis and characterisation data

N,N-diethyldithiocarbamato(trimethylphosphite)copper(I)

(1). To a stirred solution of CuCl (2.40 g, 24.0 mmol) in dry benzene (80 cm³) was added approx. three equiv. of P(OMe)₃ (8.5 cm³, 72.1 mmol), which was left to stir overnight. Slight traces of remaining CuCl suspension were removed by filtration, to remove a clear colourless solution. On addition of two-fold excess of powdered solid NaEt₂NCS₂ (8.5 g, 49.6 mmol), the solution gradually became yellow and was left to stir for 4 h after which it was filtered. The benzene was then removed *in vacuo* to leave a viscous clear yellow residue. Upon standing for several days, small transparent crystals formed. Yield 0.87 g (10.7%). Mp 70.5 °C. ¹H NMR δ (ppm) 3.69 (br. s (unresolved q), 4H, NCH₂CH₃), 3.60 (d, ³*J*_{H-P} = 11.34 Hz, 9H, POCH₃), 1.04 (br. s (unresolved t), 6H, NCH₂CH₃). ¹³C NMR δ (ppm) 206.70 (1C, NCS₂), 50.79 (3S, POCH₃), 47.24 (2C, NCH₂CH₃), 12.41 (2C, NCH₂CH₃). ³¹P NMR δ (ppm) 128.65 (br. s, 1P, Cu–P(OMe)₃). Elemental analysis, calc. for C₈H₁₉CuNO₃PS₂: C, 28.6; H, 5.7; N 4.1%; Found: C, 26.9; H, 5.6; N, 3.5%.

N,N-diethyldithiocarbamato(trimethylphosphine)copper(I)

(2). To a warm dull yellow solution of CuCl (1.33 g, 13.4 mmol) in acetonitrile (25 cm³) was added two equiv. of PMe₃ (2.8 cm³, 26.9 mmol) which, after cooling to room temperature, became a clear pale green solution. Subsequent addition of a slight excess of NaEt₂NCS₂ (2.46 g, 14.4 mmol) dissolved in acetonitrile (20 cm³) caused the solution to become a dark yellow colour with a yellow precipitate. After removal of acetonitrile *in vacuo*, a condenser was fitted and hexane (50 cm³) was added. The yellow product was slightly soluble in hexane. The mixture was gently warmed and filtered to another flask *via* cannula, in where the product could be seen to gradually precipitate as small crystals. This process was repeated with another four portions of hexane (~20 cm³ each) and the combined filtrates were then cooled to −25 °C, to allow further re-crystallisation. The mixture was filtered and the crystals were washed with three portions of pentane (~20 cm³) and dried under vacuum. The volume of the supernatant was reduced by approx. half *in vacuo* with gentle warming. The

remaining solution was again cooled to +4 °C to yield a further crop of crystals. Yield 1.32 g (34.1%). Mp 67 °C. ¹H NMR δ (ppm) 3.79 (br. s. unresolved q), 4H, NCH₂CH₃), 1.09 (br. s. (unresolved t), 6H, NCH₂CH₃), 1.02 (d, ²*J*_{H-P} = 4.72 Hz, 9H, PCH₃). ¹³C NMR δ (ppm) 47.79 (2C, NCH₂CH₃), 16.34 (d, ¹*J*_{C-P} = 58.3 Hz, 3C, PCH₃), 12.70 (2C, NCH₂CH₃). ³¹P NMR δ (ppm) 45.94 (br. s, 1P, Cu–PMe₃). Elemental analysis, calc. for C₈H₁₉CuNPS₂: C, 33.4; H, 6.7; N 4.8%; Found: C, 34.3; H, 7.1; N, 4.6%.

N,N-diethyldithiocarbamato(triethylphosphine)copper(I) (3)

To a clear colourless solution of CuCl(PET₃)₂ (10.06 g, 30 mmol) in dry benzene (75 cm³) was added ~1 equiv. of powdered solid NaEt₂NCS₂ (5.22 g, 30.5 mmol), causing it to gradually become pale yellow in colour. After stirring for ~20 h, the colour had deepened with a fine suspension precipitating. This was filtered off to leave a clear yellow solution. The solvent was removed under vacuum to clear a yellow viscous residue, to which addition of pentane (40 cm³) failed to precipitate any solid. However, clear yellow crystals precipitated from the viscous residue after standing for several days following the removal of the pentane *in vacuo*. Yield 1.45 g (14.6%). Mp ~ 69 °C. ¹H NMR δ (ppm) 3.79 (br. s. (unresolved q), 4 H, NCH₂CH₃), 1.41 (m (split q), ²*J*_{H-P} = 4.78 Hz, 6H, NCH₂CH₃), 1.09 (m) is actually two overlapping signals at 1.11 (t, 9H, PCH₂CH₃) and 1.08 (t, 6H, NCH₂CH₃). ¹³C NMR δ (ppm) 207.44 (1C, NCS₂), 47.61 (2C, NCH₂CH₃), 18.24 (d, ¹*J*_{C-P} = 57.0 Hz, 3C, PCH₂CH₃), 12.55 (2C, NCH₂CH₃), 8.56 (3C, PCH₂CH₃). ³¹P NMR δ (ppm) 8.66 (br. s, 1P, Cu–PET₃). Elemental analysis, calc. for C₁₁H₂₅CuNPS₂: C, 40.0; H, 7.6; N 4.2%; Found: C, 40.2; H, 7.7; N, 4.2%.

O-Ethylxanthato(trimethylphosphite)copper(I) (4). To a suspension of CuBr (1.04 g, 7.24 mmol) in dry toluene (~50 cm³) was added ~1 equiv. of P(OMe)₃ (~0.9 cm³) which became clear, colourless solution after ~10–15 mins of stirring, to which was slowly added ~1 equiv. of solid KEtOCS₂ (1.17 g, 7.30 mmol), causing the solution to gradually become bright yellow with a faint suspension. After stirring for 3–5 mins, a thicker, deep amber coloured suspension formed, which was redissolved on addition of a further 1 equiv. of P(OMe)₃, to give the bright lime-green/yellow solution with traces of fine

suspension After stirring over night, the solution was filtered and subsequent removal of solvents *in vacuo* initially left a orange/amber syrup in which a solid amber precipitate formed, but eventually a dry, bright yellow solid remained. The solid was washed with $3 \times 5 \text{ cm}^3$ portions of dry pentane and dried thoroughly under vacuum. The freshly prepared solid product would re-dissolve in aromatic solvents, was soluble in chlorinated hydrocarbons and was insoluble in ether and alkanes. However, after standing for several days, it could only be re-dissolved if some more P(OMe)_3 was added to the solvent. The product became slightly more amber coloured upon standing in air. Yield 1.43 g (70.9%). Mp 127.5 °C. $^1\text{H NMR } \delta$ (ppm) 4.44 (q, 2H, $\text{CH}_3\text{CH}_2\text{O}$), 3.49 (s, >9H, CH_3OP) and 1.06 (t, 3H, $\text{CH}_3\text{CH}_2\text{O}$). $^{13}\text{C NMR } \delta$ (ppm) 227.80 (1C, OCS_2), 69.03 (1C, $\text{CH}_3\text{CH}_2\text{O}$), 50.65 (>3C, CH_3OP) and 14.07 (1C, CH_3CH_2). $^{31}\text{P NMR } \delta$ (ppm) 3.87 (s, free P(OMe)_3) and 1.30 (s, 1P, Cu-P(OMe)_3). Mass spectrum (FAB) m/z 922, 800, 551 ($\text{Cu}_3(\text{EtOCS}_2)_3(\text{P(OMe)}_3)_n$; $n = 3, 2, 0$ respectively); 617 ($\text{Cu}_2(\text{EtOCS}_2)_2(\text{P(OMe)}_3)_2$); 559, 435, 311, 187 ($\text{Cu(P(OMe)}_3)_n$; $n = 4, 3, 2, 1$, respectively). Elemental analysis, calc. for $\text{C}_6\text{H}_{14}\text{CuO}_4\text{PS}_2$: C, 23.3; H, 4.6%; Found: C, 23.3; H, 4.6%.

O-ethylxanthato(trimethylphosphine)copper(i) (5). To solid $\text{CuCl(PMe}_3)_3$ (1.30 g, 3.97 mmol) and ~1 equiv. of solid KEtOCS_2 (0.66 g, 4.11 mmol) was added dry benzene (~60 cm^3), which after stirring over night, gave a bright yellow solution with traces of very faint pale suspension. After filtration, removal of solvents *in vacuo* left a bright yellow solid that was washed with $3 \times 5 \text{ cm}^3$ portions of dry pentane and dried thoroughly under vacuum. As with compound (4), this product also became slightly more amber coloured upon standing in air and was only soluble in aromatic solvents if freshly prepared or, after several days standing, some extra ligand (*i.e.* PMe_3) was added to the solvent. An attempt to sublime the solid with heating (~130 °C) under reduced pressure was unsuccessful and caused the solid to become beige in colour, although it reverted to the yellow/amber colour on cooling. Yield 0.17 g (16.5%). Mp ~ 123.5 °C. $^1\text{H NMR } \delta$ (ppm) 4.48 (q, 2H, $\text{CH}_3\text{CH}_2\text{O}$), 1.40 (t, 3H, $\text{CH}_3\text{CH}_2\text{O}$) and 1.26 (d, $^2J_{\text{H-P}} = 5.44 \text{ Hz}$, pH, PCH_3). $^{13}\text{C NMR } \delta$ (ppm) 69.47 (1C, $\text{CH}_3\text{CH}_2\text{O}$), 15.97 (d, $^1J_{\text{C-P}} = 72.16 \text{ Hz}$, 3C, PCH_3) and 14.21 (1C, $\text{CH}_3\text{CH}_2\text{O}$). $^{31}\text{P NMR } \delta$ (ppm) 39.63 (br. s, 1P, Cu-PMe_3). Elemental analysis, calc. for $\text{C}_6\text{H}_{14}\text{CuOPS}_2$: C, 27.6; H, 5.4%; Found: C, 27.7; H, 5.2%.

Acknowledgements

The authors would like to thanks EPSRC, UK for financial assistance. This paper was written whilst POB was a Distinguished Visiting Fellow at the Institute of Advanced Study, Durham University. He thanks the Institute and the University for their hospitality and support. M. A. would like to thank Center of Research Excellence in Renewable Energy, KFUPM for the support.

References

- (a) D. Cocouvanis, *Prog. Inorg. Chem.*, 1979, **26**, 301; (b) A. M. Bond and R. L. Martin, *Coord. Chem. Rev.*, 1984, **54**, 23; (c) A. M. Bond, A. R. Hendrickson, R. L. Martin, J. E. Moir and D. R. Page, *Inorg. Chem.*, 1983, **22**, 3440; (d) N. Robertson and L. Cronin, *Coord. Chem. Rev.*, 2002, **227**, 93; (e) A. Kobayashi, E. Fujiwara and H. Kobayashi, *Chem. Rev.*, 2004, **104**, 5243; (f) M. Bousseau, L. Valade, J.-P. Legros, P. Cassoux, M. Garbaukas and L. V. Interrante, *J. Am. Chem. Soc.*, 1986, **108**, 1908; (g) L. I. Victoriano, *Polyhedron*, 2000, **19**, 2269.
- (a) S.-W. Lai, M. G. B. Drew and P. D. Beer, *J. Organomet. Chem.*, 2001, **637-639**, 89; (b) P. D. Beer, N. Bery, M. G. B. Drew, O. D. Fox, M. E. Padilla-Tosta and S. Patell, *Chem. Commun.*, 2001, 199; (c) W. W. H. Wong, J. Cookson, E. A. L. Evans, E. J. L. McInnes and P. D. Beer, *Chem. Commun.*, 2005, 2214; (d) F. W. B. Einstain and J. S. Field, *Acta Crystallogr., Sect. B: Struct. Crystallogr. Cryst. Chem.*, 1974, **30**, 2928.
- W. E. Hatfield, P. Singh and F. Nepveu, *Inorg. Chem.*, 1990, **29**, 4241.
- A. M. M. Lanfredi, F. Ugozzoli and A. Camus, *J. Chem. Crystallogr.*, 1996, **26**, 141.
- J. J. Steggerda, J. A. Cras and J. Willemse, *Recl. Trav. Chim. Pays-Bas*, 1981, **100**, 41.
- L. I. Victoriano and H. B. Cortes, *J. Coord. Chem.*, 1996, **39**, 231.
- J. P. Fackler, R. J. Staples, C. W. Liu, R. T. Stubbs, C. Lopez and J. T. Pitts, *Pure Appl. Chem.*, 1998, **70**, 839.
- L. M. Nguyen, M. E. Dellinger, J. T. Lee, R. A. Rheingold and R. D. Pike, *Inorg. Chim. Acta*, 2005, **358**, 1331.
- A. Kumar, H. Mayer-Figge, W. S. Sheldrick and N. Singh, *Eur. J. Inorg. Chem.*, 2009, 2720.
- A. O. Gorgulu, M. Arslan and E. Cil, *J. Coord. Chem.*, 2005, **58**, 1225.
- C. Kowala and J. M. Swan, *Aust. J. Chem.*, 1966, **19**, 555.
- H. T. Brinkhoff, A. G. Matthijssen and C. G. Oomes, *Inorg. Nucl. Chem. Lett.*, 1971, **7**, 87.
- A. M. Bond and R. L. Martin, *Coord. Chem. Rev.*, 1984, **54**, 23.
- J. Willemse, J. A. Cras, J. J. Stegger and C. P. Keyzers, *Struct. Bonding.*, 1976, **28**, 83.
- J. J. Steggerda, J. A. Cras and J. Willemse, *Rec. J. Royal Netherlands Chem. Soc.*, 1981, **100**, 41.
- (a) D. Cardell, G. Hogarth and S. Faulkner, *Inorg. Chim. Acta*, 2006, **359**, 1321; (b) G. Hogarth, *Prog. Inorg. Chem.*, 2005, **53**, 71 and references therein.
- K. Xu, W. Ding and Y. Chen, *J. Chem. Crystallogr.*, 2004, **34**, 665.
- G. F. Han, X. J. Yang, L. D. Lu and X. Wang, *Polish J. Chem.*, 2004, **78**, 27.
- M. M. Khwaja, T. J. Cardwell and R. J. Magee, *Anal. Chim. Acta*, 1973, **64**, 9.
- G. W. Watt and B. J. McCormick, *Spectrochim. Acta*, 1965, **21**, 753.
- K.-M. Chi, J. Farkas, M. J. Hampden-Smith, T. T. Kodas and E. N. Duesler, *J. Chem. Soc., Dalton Trans.*, 1992, 3111.
- H.-K. Shin, M. J. Hampden-Smith, T. T. Kodas and E. N. Duesler, *Polyhedron*, 1991, **10**, 645.
- K.-M. Chi, T. S. Corbitt, M. J. Hampden-Smith, T. T. Kodas and E. N. Duesler, *J. Organomet. Chem.*, 1993, **449**, 181.
- M. Chunggaze, M. A. Malik, P. O'Brien, A. J. P. White and D. J. Williams, *J. Chem. Soc., Dalton Trans.*, 1998, 3839.
- M. Hong, Q. Zhang, R. Cao, D. Wu, J. Chen, H. Zhang, H. Liu and J. Lu, *Inorg. Chem.*, 1997, **36**, 6251.
- A. J. Vreugdenhil, S. H. R. Brienne, I. S. Butler, J. A. Finch and R. D. Markwell, *Spectrochim. Acta, Part A*, 1997, **53**, 2139.
- A. I. Said, *Transition Met. Chem.*, 1992, **17**, 130.
- A. A. M. Aly, *Transition Met. Chem.*, 1991, **16**, 249-251.